$^{99m}Tc(CO)_3$(NTA) and ^{131}I-OIH: Comparable Plasma Clearances in Patients with Chronic Kidney Disease

Andrew T. Taylor[1], Malgorzata Lipowska[1], and Hui Cai[2]

[1]*Department of Radiology and Imaging Sciences, Emory University, Atlanta, Georgia; and* [2]*Department of Medicine and Physiology, Emory University, Atlanta, Georgia*

The pharmacokinetics of the tricarbonyl core radiopharmaceutical $^{99m}Tc(CO)_3$-nitrilotriacetic acid ($^{99m}Tc(CO)_3$(NTA)) in rats and subjects with normal renal function are comparable to those of ^{131}I-*o*-iodohippuran (^{131}I-OIH), the radiopharmaceutical gold standard for the measurement of effective renal plasma flow. Our objective was to compare the pharmacokinetics of these 2 tracers in subjects with renal failure. **Methods:** $^{99m}Tc(CO)_3$(NTA) was prepared with commercially available NTA and a commercially available labeling kit and isolated by reversed-phase high-performance liquid chromatography. Approximately 74 MBq (2.0 mCi) of $^{99m}Tc(CO)_3$(NTA) were coinjected with approximately 11.1 MBq (300 μCi) of ^{131}I-OIH in 8 subjects with stage 3–4 renal failure; simultaneous images were obtained for 24 min, followed by an anterior image over the gallbladder and abdomen. Plasma clearances were determined from 10 blood samples obtained 3–180 min after injection using the single-injection, 2-compartment model. Plasma protein binding, red cell uptake, and percentage injected dose in the urine at 30 and 180 min were determined. **Results:** There was no difference in the plasma clearances of $^{99m}Tc(CO)_3$(NTA) and ^{131}I-OIH (177 ± 63 vs. 171 ± 66 mL/min/1.73 m^2, respectively) ($P = 0.41$). The plasma protein binding and red cell uptake of $^{99m}Tc(CO)_3$(NTA) were 35% ± 7% and 6% ± 3%, respectively; both values were significantly lower than the plasma protein binding (71% ± 5%) and red cell uptake (16% ± 2%) of ^{131}I-OIH ($P < 0.001$). There was no significant difference in the percentage injected dose in the urine at 30 min ($P = 0.24$) and at 3 h ($P = 0.82$); for comparison, the percentage dose in the urine at 3 h was 77% ± 9% for $^{99m}Tc(CO)_3$(NTA) and 78% ± 11% for ^{131}I-OIH. Image quality with $^{99m}Tc(CO)_3$(NTA) was excellent and no activity was identified in the gallbladder or intestine. **Conclusion:** Results in patients with renal failure show the clearance and rate of urine excretion of $^{99m}Tc(CO)_3$(NTA) to be equivalent to that of ^{131}I-OIH.

Key Words: chronic kidney disease; renal radiopharmaceuticals; $^{99m}Tc(CO)_3$(NTA); ^{131}I-ortho-iodohippurate (^{131}I-OIH); ^{99m}Tc-mercaptoacetyltriglycine (^{99m}Tc-MAG3)

J Nucl Med 2013; 54:578–584
DOI: 10.2967/jnumed.112.108357

Orthoiodohippuran labeled with ^{131}I (^{131}I-OIH) has been recognized as the radiopharmaceutical standard for the measurement of effective renal plasma flow (*1*). ^{131}I-OIH is primarily extracted by the renal tubules and has excellent pharmacokinetic properties, with a clearance only slightly less than that of *p*-aminohippuran, but its use has been compromised by the suboptimal imaging characteristics of the 364-keV photon of ^{131}I and the delivery of relatively high radiation doses to kidneys and thyroid in patients with impaired renal function (*1–3*). These limitations resulted in a search for a ^{99m}Tc tracer with properties comparable to ^{131}I-OIH and led to the subsequent development and widespread use of ^{99m}Tc-mercaptoacetyltriglycine (^{99m}Tc-MAG3) (*4,5*), which is now used in an estimated 70% of all the renal scans in the United States.

Despite its widespread use, however, ^{99m}Tc-MAG3 still has limitations. A small percentage of ^{99m}Tc-MAG3 is eliminated via the hepatobiliary pathway; this percentage increases with reduced renal function, and gallbladder activity has been mistaken for activity in the kidney (*6–9*). In addition, the clearance of ^{99m}Tc-MAG3 is only 50%–60% of that of ^{131}I-OIH (*1,5,10,11*); this limitation has led some investigators to conclude that ^{99m}Tc-MAG3 is not suitable for the measurement of effective renal plasma flow (*10*). The reproducibility of the ^{99m}Tc-MAG3 clearance based on plasma sample measurements has also been questioned. Kotzerke et al. presented data suggesting that ^{99m}Tc-MAG3 clearance was not precise enough to evaluate a change in kidney function (*12*), and Piepsz et al. have reported marked variations in repeated ^{99m}Tc-MAG3 plasma clearance measurements and have warned that changes in the ^{99m}Tc-MAG3 plasma clearance should be interpreted with caution (*13*).

These limitations stimulated continuing efforts to develop a ^{99m}Tc renal radiopharmaceutical with both reduced hepatobiliary excretion and superior pharmacokinetic properties that would allow a more accurate and precise measurement of effective renal plasma flow. For almost 20 y, these synthetic efforts exclusively used the $\{TcO\}^{3+}$ core with technetium in its +5 oxidation state, but more recently, synthetic efforts have shifted to take advantage of the ^{99m}Tc water-stable organometallic tricarbonyl precursor, $[^{99m}Tc(CO)_3(H_2O)_3]^+$, with its *fac*-$\{^{99m}Tc(CO)_3\}^+$ core and ^{99m}Tc in a +1 oxidation state (*14–19*).

Received May 7, 2012; revision accepted Oct. 15, 2012.
For correspondence or reprints contact: Andrew T. Taylor, Department of Radiology and Imaging Sciences, Emory University, Atlanta, GA 30322.
E-mail: ataylor@emory.edu
Published online Feb. 19, 2013.

^{99m}Tc-tricarbonyl-nitrilotriacetic acid, ^{99m}Tc(CO)$_3$(NTA), is formed as a single species; it is a stable, dianionic complex at physiologic pH and has a dangling carboxylate group favoring tubular transport (*17*). Initial studies in Sprague–Dawley rats and subjects with normal renal function demonstrated that ^{99m}Tc(CO)$_3$(NTA) has pharmacokinetic properties comparable to those of ^{131}I-OIH (*17,18*); however, results in subjects with normal renal function do not necessarily predict the pharmacokinetics in patients with renal failure. A decreased renal function impairs the excretion of the renal tracer ^{99m}Tc-CO$_2$-DADS (DADS = *N,N′*-bis (mercaptoacetyl)-2,3-diaminopropanoate) to a greater extent than that of ^{131}I-OIH (*9,20*), and ^{99m}Tc-MAG3 demonstrates increased biliary and intestinal activity in rats and patients with renal failure, compared with healthy controls (*9,20,21*). This study was initiated to determine the effect of chronic kidney disease on the relative pharmacokinetic properties of ^{99m}Tc(CO)$_3$(NTA) and ^{131}I-OIH.

MATERIALS AND METHODS

General

NTA was purchased from Aldrich. ^{99m}Tc-pertechnetate ($^{99m}TcO_4^-$) was eluted from a ^{99}Mo/^{99m}Tc generator (Amersham Health) with 0.9% saline. IsoLink vials were obtained as a gift from Covidien. [^{99m}Tc(CO)$_3$(H$_2$O)$_3$]$^+$ was prepared according to the manufacturer's insert by adding $^{99m}TcO_4^-$ generator eluent (1 mL; 1.11–3.7 GBq [30–100 mCi]) to the IsoLink vial, heating for 30 min at 100°C, and adding 1N HCl (120 μL) to neutralize the solution. The radiolabeled compound was analyzed on a high-performance liquid chromatography (HPLC) instrument (System Gold Nouveau; Beckman Coulter) equipped with a model 170 radiometric detector and a model 166 ultraviolet light–visible light detector, 32 Karat chromatography software (Beckman Coulter), and an octyldecyl silane column (C18 RP Ultrasphere; 5-μm, 4.6 × 250 mm [Beckman Coulter]). The solvent system was 0.05 M triethylammonium bicarbonate buffer, pH 2.5 (solvent A) and ethanol (solvent B), and the flow rate was 1 mL/min. The gradient method was the same as reported previously (*16*). Urine, plasma, and red blood cell radioactivity were measured with a γ-counter (Packard Cobra II γ-Counter; Perkin Elmer) with correction for ^{131}I scatter into the ^{99m}Tc window.

Radiosynthesis of ^{99m}Tc(CO)$_3$(NTA) and ^{131}I-OIH

The NTA ligand was labeled as previously described (*17,22*). Briefly, 0.5 mL of a freshly prepared solution of the [^{99m}Tc(CO)$_3$(H$_2$O)$_3$]$^+$ precursor (pH ~7–8) was added to a vial containing approximately 1.0 mg of the NTA ligand in 0.2 mL of water. The pH of the solution was adjusted to approximately 7 with 1 M NaOH, heated at 70°C for 15 min, and cooled to room temperature, yielding the dianion *fac*-[^{99m}Tc(CO)$_3$(NTA)]$^{2-}$, which we describe as ^{99m}Tc(CO)$_3$(NTA). ^{99m}Tc(CO)$_3$(NTA) was separated from unlabeled ligand by HPLC; the radiochemical purity was greater than 99%. Ethanol was partially removed by N_2 gas, and the collected solution of ^{99m}Tc(CO)$_3$(NTA) was buffered in physiologic phosphate-buffered saline at pH 7.4. The HPLC-purified complex in phosphate-buffered saline (pH 7.4) was passed through a Sep-Pak Plus C_{18} cartridge (Waters Co.) (primed with 4 mL of ethanol) and sterile Millex-GS 22-μm filter (Millipore Co.) (primed with 4 mL of saline) into a sterile, pyrogen-free empty vial. The final concentration was 37 MBq/mL (1 mCi/mL), and the final pH was 7.4. Test samples were sent for analysis and determined to be sterile and pyrogen-free.

^{131}I-OIH was prepared by the isotope-exchange reaction between nonradioactive hippuran (OIH) and radioactive sodium iodide (Na^{131}I) according to the method reported by Anghileri (*23*) and modified as previously described (*17*). ^{131}I-OIH was obtained with a 98%–99% labeling yield.

Patient Studies

All studies were performed with the approval of the Radioactive Drug Research Committee and the Emory University Institutional Review Board; signed consent was obtained from each subject. The study population consisted of 8 subjects (5 men, 3 women; mean age, 64.3 ± 10 y) initially diagnosed with stage 3–4 chronic kidney disease. In addition to chronic kidney disease, 8 of the subjects were diagnosed with hypertension: 5 with type 2 diabetes, 4 with coronary artery disease, 3 with gout, and 3 with hyperlipidemia or hypercholesterolemia. The glomerular filtration rate (GFR in mL/min/1.73 m^2) was determined for each patient using the Modification of Diet in Renal Disease (MDRD) formula and the most recently available serum creatinine measurement (*24*). Pregnancy was excluded by means of a urine pregnancy test. Each patient was monitored during the study, and measurements of blood pressure, heart rate, and temperature were obtained before and after injection for each subject. After the coinjection of approximately 74 MBq (~2 mCi) of ^{99m}Tc(CO)$_3$(NTA) and approximately 11.1 MBq (300 μCi) of ^{131}I-OIH, imaging was performed for 24 min using an Infinia camera (GE Healthcare) with a 9.5-mm (3/8-in) crystal fitted with a high-energy collimator; a 20% window was centered over the 365-keV photopeak of ^{131}I, and a second 20% window was centered over the 140-keV photopeak of ^{99m}Tc. At the conclusion of the 24-min acquisition, a postvoid image of the kidneys and an anterior image over the gallbladder and abdomen were obtained. Data were acquired in a 128 × 128 matrix using a 3-phase dynamic acquisition and processed on a Xeleris computer (GE Healthcare) with an extensive in-house upgrade of the original QuantEM renal software (GE Healthcare). Renogram curves were generated using cortical (parenchymal) and whole-kidney regions of interest (ROIs). Blood samples were obtained at 3, 5, 10, 20, 30, 45, 60, 90, 120, and 180 min after injection, and plasma clearances for ^{131}I-OIH and ^{99m}Tc(CO)$_3$(NTA) were determined using the single-injection, 2-compartment model of Sapirstein et al. (*25*). The volunteers voided at 30 and 180 min after injection to determine the percentage dose in the urine. Plasma protein binding (PPB) was determined by ultracentrifugation (Centrifree micropartition system; Amicon Inc.) of 1 mL of plasma: PPB = (1.0 – [ultrafiltrate concentration/plasma concentration]) × 100. The percentage uptake in the erythrocytes was calculated from the whole blood (counts/g) and packed cells (counts/g) using the following equation: [(counts/g in erythrocytes × hematocrit)/counts/g in whole blood]. No correction was made for plasma trapped in the red blood cell sample. PPB and erythrocyte uptake were calculated using duplicate samples, and the mean values were reported.

Statistical Analysis

All results are expressed as the mean ± SD. To determine the statistical significance of differences between the 2 groups, comparisons were made with the 2-tailed Student *t* test for paired data; a *P* value of less than 0.05 was considered to be statistically significant.

RESULTS

The plasma clearance of ^{99m}Tc(CO)$_3$(NTA) averaged 177 ± 63 (SD) mL/min/1.73 m^2, compared with 171 ± 66

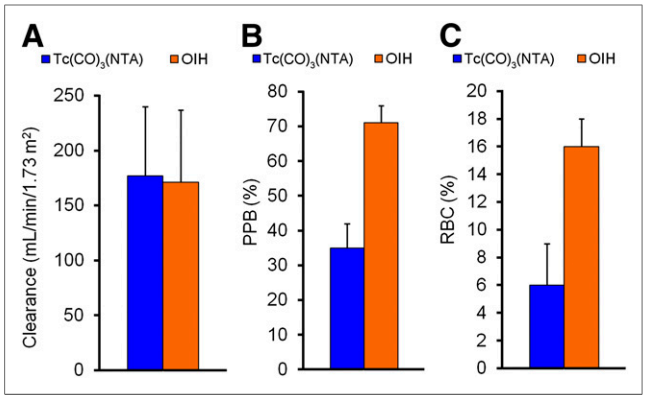

FIGURE 1. Bar graphs comparing clearance (A), PPB (B), and red cell uptake (RBC) (C) of ^{99m}Tc(CO)$_3$(NTA) and ^{131}I-OIH in 8 subjects with chronic kidney disease.

mL/min/1.73 m^2 for ^{131}I-OIH (Fig. 1; Table 1). The PPB of ^{99m}Tc(CO)$_3$(NTA), 35% ± 7%, was significantly less than that of ^{131}I-OIH, 71% ± 5% ($P < 0.001$); similarly, red cell uptake for ^{99m}Tc(CO)$_3$(NTA), 6% ± 3%, was also significantly less than that of ^{131}I-OIH, 16% ± 2% ($P < 0.001$) (Fig. 1; Table 1). There was no significant difference in the urine excretion of ^{99m}Tc(CO)$_3$(NTA) and ^{131}I-OIH at 30 or 180 min ($P = 0.24$ and 0.82, respectively) (Fig. 2; Table 2).

The image quality of ^{99m}Tc(CO)$_3$(NTA) was superior to that of ^{131}I-OIH. A representative study is illustrated in Figure 3. There was no significant difference in relative uptake (55.3% ± 9.0% for ^{99m}Tc(CO)$_3$(NTA) in the left kidney, compared with 55.5% ± 8.1% for ^{131}I-OIH; $P = 0.79$). Although the renogram curves for ^{99m}Tc(CO)$_3$(NTA) and ^{131}I-OIH were comparable, the ^{131}I-OIH renograms curves were quite noisy and measurements of time to peak and 20-min-to-maximum ratios for whole-kidney and cortical ROIs were not obtained. Finally, no gallbladder or intestinal activity was identified on the anterior images obtained at 30 min over the gallbladder and abdomen for any of the subjects.

DISCUSSION

The plasma clearance of ^{99m}Tc(CO)$_3$(NTA) was the same as that of ^{131}I-OIH in healthy volunteers (*18*), and identical results were obtained in subjects with chronic kidney disease; renal failure did not diminish the clearance of ^{99m}Tc(CO)$_3$(NTA) out of proportion to ^{131}I-OIH as has been described with previous tracers (*20*). In addition, no ^{99m}Tc(CO)$_3$(NTA) activity was identified in the gallbladder or intestine on anterior images obtained approximately 30 min after injection. This result is in contrast to ^{99m}Tc-MAG3, where renal failure can result in hepatobiliary excretion (*6–9*). The ^{99m}Tc(I)(CO)$_3$(NTA) complex is significantly smaller than the ^{99m}Tc(V)O-MAG3 complex, and its smaller 3-dimensional configuration appears to have less affinity for the hepatobiliary transport system than the larger 3-dimensional configuration of the ^{99m}Tc(V)O-MAG3 complex. The renal extraction fraction of ^{99m}Tc(CO)$_3$(NTA) was not directly measured, but it can be inferred to be higher than the 40%–60% extraction fraction of ^{99m}Tc-MAG3 because ^{99m}Tc(CO)$_3$(NTA) has a more rapid clearance. For comparison, the extraction fraction of ^{99m}Tc-diethyltriaminepentaacetic acid (^{99m}Tc-DTPA) is approximately 20% (*1*).

The clearance of ^{99m}Tc-MAG3 is proportional to the GFR (*26*), and the same relationship is likely to apply for ^{99m}Tc(CO)$_3$(NTA). Interestingly, both the ^{99m}Tc(CO)$_3$(NTA) and the ^{131}I-OIH clearances of subject 3 (295 and 297 mL/min/1.73 m^2, respectively) seem unexpectedly high given the subject's relatively low MDRD GFR of 39 mL/min/1.73 m^2 (Table 1). The explanation for this higher clearance may be due to the fact that this particular female subject had type 2 diabetes and was quite obese (109 kg); compared with isotopic clearance methods, the MDRD equation significantly underestimates the GFR in obese individuals with type 2 diabetes (*27*). Conversely, the MDRD GFR of subject 4 (67 mL/min/1.73 m^2) is higher than might be expected given the ^{99m}Tc(CO)$_3$(NTA) and ^{131}I-OIH clearances of 159 and 158 mL/min/1.73 m^2, respectively. This particular

TABLE 1
GFR, Clearance, PPB, and Red Cell Uptake for ^{99m}Tc(CO)$_3$(NTA) and ^{131}I-OIH

		NTA			OIH			
Patient	GFR*	Clearance*	PPB (%)	RBC (%)	Clearance*	PPB (%)	RBC (%)	NTA/OIH clearance (%)
1	25	186	43	8	187	77	18	99
2	53	215	39	10.5	196	73	17	110
3	39	295	43	4.8	297	76	16	99
4	67	159	26	3	158	66	13	101
5	62	200	37	7.2	187	73	17	107
6	17	84	25	9.1	85	64	18	99
7	26	144	33	3.3	168	68	15	86
8	34	134	32	4.8	93	67	15	143
Mean ± SD		177 ± 63	35 ± 7	6 ± 3	171 ± 66	71 ± 5	16 ± 2	106 ± 17

*GFR, ^{99m}Tc(CO)$_3$(NTA), and ^{131}I-OIH clearances are expressed in mL/min/1.73 m^2; GFR was calculated using MDRD formula (*24*).
RBC = red cell uptake.

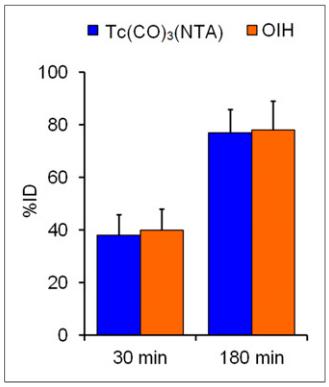

FIGURE 2. Bar graphs comparing urine excretion of $^{99m}Tc(CO)_3(NTA)$ and ^{131}I-OIH at 30 and 180 min in 8 subjects with chronic kidney disease. %ID = percentage injected dose.

subject was thin, was 74 y of age, and probably had sarcopenia; the decreased muscle mass likely resulted in a lower serum creatinine, leading to an overestimation of the true GFR by the MRDR equation.

The results also confirm our initial observations that $^{99m}Tc(CO)_3(NTA)$ has lower protein binding and red cell binding than does ^{131}I-OIH (*18*). Lower protein binding may increase the extraction fraction because unbound tracer can be filtered by the glomerulus and extracted by the tubules. In addition, the reduction in red cell binding is an advantage in obtaining an accurate measure of extraction fraction; the extraction fraction is based on the difference in the plasma concentration of the tracer in arterial and renal venous blood. The tracer bound to red cells is in equilibrium with the plasma; when a renal vein blood sample is obtained, tracer associated with the red cells reequilibrates with the plasma before the plasma can be separated from the red cells and results in an overestimation of the plasma tracer concentration.

The difference in the relative height of the cortical curves in Figure 3 is due to the differences in the size of the relative cortical ROIs. The function of the cortical curve is to display the transit time through the cortex without contaminating the curve because of retained activity in the collecting system; the cortical (parenchymal) ROIs are not drawn to have equal areas but to exclude the renal pelvis (*28*). In general, a cortical ROI with a larger area will have more counts than a contralateral cortical ROI with a smaller area; consequently, the renogram curve with the larger cortical ROI will have a greater maximum. It is the shape of the cortical renogram curve that is important, not the absolute height.

NTA is widely present in drinking water, primarily as metal complexes rather than a free acid (*29–32*), and has been shown to have a good safety profile. On the basis of the available studies, Health Canada has determined the maximum acceptable level of NTA in drinking water to be 0.4 mg/L (*30*). The kinetics and metabolism of the NTA ligand have been investigated in several species, including humans (*29–32*); in our studies, no free NTA ligand was injected because the ligand was separated from the $^{99m}Tc(CO)_3(NTA)$ complex by HPLC before injection. Free NTA ligand would undoubtedly be injected in a kit formulation, but the injected dose of NTA would probably still be below the daily acceptable limit established by Health Canada. In our studies, the administered dose of the $^{99m}Tc(CO)_3(NTA)$ complex was extremely small and did not exceed 0.03 μg, an amount far below the acceptable level in a liter of drinking water. In our previous study of subjects with normal renal function, we found no evidence of toxicity or pharmacologic effect based on patient monitoring, vital signs, urine analysis, complete blood count, and chemistry panels obtained before and after $^{99m}Tc(CO)_3(NTA)$ administration (*18*), and there was no evidence of any effect in this study based on the monitoring of vital signs and the subjects' responses before and after injection.

The ^{131}I-OIH renogram curves are too noisy to calculate reliable time-to-peak measurements and 20-min–to–maximum count ratios for whole-kidney results. First, the subjects received only approximately 11.1 MBq (300 μCi) of ^{131}I-OIH; even though this is the standard imaging dose for ^{131}I-OIH renal scans, it is considerably less than the 74-MBq (~2-mCi) administered amount of $^{99m}Tc(CO)_3(NTA)$. Second, all the subjects had reduced renal function, with a mean ^{131}I-OIH plasma clearance of 198 mL/min (171 mL/min/1.73 m^2), compared with the normal ^{131}I-OIH clearance of 472–530 mL/min (*5,18*). The fact that renal function was reduced by approximately 60% substantially reduced the counting rate in the renal and parenchymal ROIs. Even so, ^{131}I-OIH studies performed in the 1980s provided renogram curves

TABLE 2
Percentage of Injected Dose in Urine of $^{99m}Tc(CO)_3(NTA)$ and ^{131}I-OIH at 30 and 180 Minutes After Injection

	30 min			180 min		
Patient	NTA (%)	OIH (%)	NTA/OIH (%)	NTA (%)	OIH (%)	NTA/OIH (%)
1	42	42	99	74	75	99
2	43	41	105	83	77	108
3	31	33	94	81	79	102
4	44	46	96	81	81	99
5	46	47	98	84	81	103
6	21	24	88	56	59	96
7	40	38	105	86	76	114
8	37	50	74	75	98	77
Mean ± SD	38 ± 8	40 ± 8	95 ± 10	77 ± 9	78 ± 11	100 ± 11

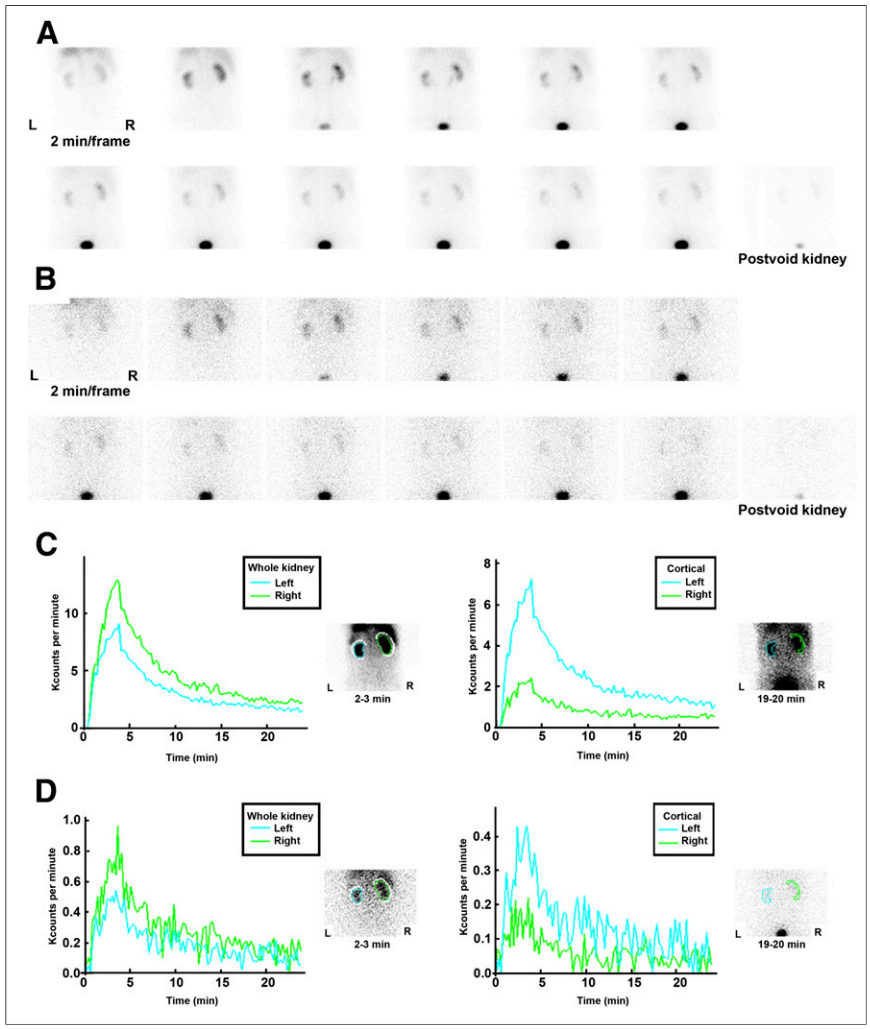

FIGURE 3. Two-minute kidney images after simultaneous injection of 95.8 MBq (2.59 mCi) of ^{99m}Tc(CO)$_3$(NTA) (A) and 11.8 MBq (0.32 mCi) of ^{131}I-OIH (B) in 74-y-old man with stage 3 chronic kidney disease. Whole-kidney and cortical (parenchymal) renogram curves are displayed in C for ^{99m}Tc(CO)$_3$(NTA) and in D for ^{131}I-OIH. Renogram curves for ^{131}I-OIH are quite noisy because of relatively low counting rate resulting from lower administered dose, poor capture of 364-keV photon of ^{131}I by 9.5-mm (3/8-in) crystal, and high-energy collimator not optimized for ^{131}I.

with sufficient counts after the administration of 11.1 MBq (300 μCi) of ^{131}I-OIH, even in patients with reduced renal function (*33*). Zuckier et al. made an observation similar to ours in a 1987 paper and demonstrated that the net counting rate for ^{131}I on their newer camera was only 27% of the counting rate on their older camera (*34*). The older camera had a thicker 12.7-mm (1/2-in) crystal, compared with the 9.5-mm (3/8-in) crystal on the newer camera; in addition, the photon energy for ^{131}I fell into the mid range of the high-energy collimator specification for the older camera whereas it fell at the extreme of the resolving capacity of the collimator of the newer camera (*34*).

In addition to the problems of acquiring low-count ^{131}I images on current γ-cameras, another potential source of error is the clearance measurement, which depends on accurately timed plasma samples and plasma volumes. Because both tracers were injected simultaneously, any error in timing or measurement of the sample volume would be contained in both datasets. Another possible criticism is the relatively small sample size. Even with a sample size of 8 subjects, the data show that the plasma clearance and urinary excretion of ^{131}I-OIH and ^{99m}Tc(CO)$_3$(NTA) are equivalent. A larger sample size would result in tighter confidence intervals but would be highly unlikely to change the conclusion.

An obvious question is how will ^{99m}Tc(CO)$_3$(NTA) compare to ^{99m}Tc-MAG3? There was no direct comparison in this study, but several conclusions can be inferred on the basis of available data. The plasma clearance of ^{99m}Tc(CO)$_3$(NTA) will be more rapid than that of ^{99m}Tc-MAG3. This conclusion is based on 2 observations: first, the ratio of ^{99m}Tc-MAG3 to ^{131}I-OIH plasma clearance is approximately 50%–60% whereas the ratio of ^{99m}Tc(CO)$_3$(NTA) to ^{131}I-OIH is approximately 100% (*1,5,10,11,18*). Second, using software designed to measure the camera-based clearance for ^{99m}Tc-MAG3 based on the percentage of the injected dose accumulated in the kidney from 1 to 2.5 min after injection (*35*), ^{99m}Tc(CO)$_3$(NTA) had a significantly higher camera-based clearance in healthy subjects than did ^{99m}Tc-MAG3, 456 ± 130 mL/min/1.73 m^2 versus 321 ± 69 mL/min/1.73 m^2, respectively (*18,35,36*). The fact that ^{99m}Tc(CO)$_3$(NTA) is cleared from the plasma and accumulates in the kidney more rapidly than

^{99m}Tc-MAG3 should lead to more robust camera clearance measurements because background correction is a source of error in camera-based clearance methods, and the higher kidney-to-background ratio obtained with ^{99m}Tc(CO)$_3$(NTA) will minimize the background correction error, particularly in patients with reduced renal function. The same factors may improve the image quality of kidneys with reduced function. Moreover, the fact that the clearance of ^{99m}Tc(CO)$_3$(NTA) is equivalent to that of ^{131}I-OIH will allow a much more direct measurement of effective renal plasma flow. Finally, ^{99m}Tc-MAG3 is recognized as being superior to ^{99m}Tc-DTPA for the diagnosis of obstruction, particularly in patients with reduced renal function (*37–40*); the superiority of ^{99m}Tc-MAG3 over ^{99m}Tc-DTPA is because ^{99m}Tc-MAG3 is cleared much more rapidly than ^{99m}Tc-DTPA. Whether the more rapid clearance of ^{99m}Tc(CO)$_3$(NTA), compared with ^{99m}Tc-MAG3, will lead to an improved diagnostic performance in patients with suspected obstruction remains to be answered and will require carefully controlled studies.

CONCLUSION

^{99m}Tc(CO)$_3$(NTA) is cleared from the blood and excreted in the urine as rapidly as ^{131}I-OIH in subjects with chronic kidney disease; moreover, no activity was noted in the gallbladder or intestines. Previous studies have shown that ^{99m}Tc(CO)$_3$(NTA) is a stable dianionic complex that is formed as a single species and is amenable to kit formulation. ^{99m}Tc(CO)$_3$(NTA) has the advantages of a lower protein binding than ^{131}I-OIH and less activity associated with red cells. These results suggest that ^{99m}Tc(CO)$_3$(NTA) will prove to be a superior ^{99m}Tc renal tubular imaging agent and a superior ^{99m}Tc tracer for the measurement of effective renal plasma flow.

DISCLOSURE

The costs of publication of this article were defrayed in part by the payment of page charges. Therefore, and solely to indicate this fact, this article is hereby marked "advertisement" in accordance with 18 USC section 1734. This research was supported by a grant from the National Institutes of Health (NIH/NIDDK R37 DK38842). Andrew T. Taylor is entitled to a share of the royalties for the use of QuantEM software for processing MAG3 renal scans, which was licensed by Emory University to GE Healthcare in 1993. He and his coworkers have subsequently developed in-house, noncommercial software, which was used in this study and could affect their financial status. The terms of this arrangement have been reviewed and approved by Emory University in accordance with its conflict-of-interest policies. No other potential conflict of interest relevant to this article was reported.

ACKNOWLEDGMENTS

We thank Angela Akbasheva, Russell Folks, Eugene Malveaux, and Liudmila Verdes for their excellent technical assistance. Covidien is gratefully acknowledged for providing the IsoLink kits.

REFERENCES

1. Eshima D, Fritzberg AR, Taylor A. Tc-99m renal tubular function agents: current status. *Semin Nucl Med.* 1990;20:28–40.
2. Marcus CS, Kuperus JH. Pediatric renal iodine-123 orthoiodohippurate dosimetry. *J Nucl Med.* 1985;26:1211–1214.
3. Burbank MK, Tauxe WN, Maher FT, Hunt JC. Evaluation of radioiodinated hippuran for the estimation of renal plasma flow. *Proc Staff Meet Mayo Clin.* 1961;36:372–386.
4. Fritzberg AR, Kasina S, Eshima D, Johnson DL. Synthesis and biological evaluation of technetium-99m MAG3 as a hipurran replacement. *J Nucl Med.* 1986; 27:111–116.
5. Taylor A, Eshima D, Fritzberg AR, Christian PE, Kasina S. Comparison of iodine-131 OIH and technetium-99m MAG3 renal imaging in volunteers. *J Nucl Med.* 1986;27:795–803.
6. Sanchez J, Friedman S, Kempf J, Abdel-Dayem H. Gallbladder activity appearing 6 minutes after the intravenous injection of Tc99m MAG3 simulating a picture of obstructive uropathy of the right kidney. *Clin Nucl Med.* 1993;18:30–34.
7. Rosen JM. Gallbladder uptake simulating hydronephrosis on Tc-99m MAG3 scintigraphy. *Clin Nucl Med.* 1993;18:713–714.
8. Shattuck LA, Eshima D, Taylor AT, et al. Evaluation of the hepatobiliary excretion of technetium-99m-MAG3 and reconstitution factors affecting radiochemical purity. *J Nucl Med.* 1994;35:349–355.
9. Taylor A Jr, Eshima D, Christian PE, et al. Technetium-99m MAG3 kit formulation: preliminary results in normal volunteers and patients with renal failure. *J Nucl Med.* 1988;29:616–622.
10. Jafri RA, Britton KE, Nimmon CC, et al. Technetium-99m MAG3: a comparison with iodine-123 and iodine-131 orthoiodohippurate in patients with renal disorders. *J Nucl Med.* 1988;29:147–158.
11. Bubeck B, Brandau W, Weber E, et al. Pharmacokinetics of technetium-99m-MAG3 in humans. *J Nucl Med.* 1990;31:1285–1293.
12. Kotzerke J, Glatz S. Grillenberger. Reproducibility of a single-sample method for ^{99m}Tc-MAG3 clearance under clinical conditions. *Nucl Med Commun.* 1997; 18:352–357.
13. Piepsz A, Tondeur M, Kinthaert J, et al. Reproducibility of technetium-99m mercaptoacetylglycine clearance. *Eur J Nucl Med.* 1996;23:195–198.
14. Lipowska M, Cini R, Tamasi G, Xu X, Taylor AT, Marzilli LG. Complexes having the *fac*-{M(CO)$_3$}$^+$ core (M = Tc, Re) useful in radiopharmaceuticals: x-ray and NMR structural characterization and density functional calculations of species containing two sp^3 N donors and one sp^3 O donor. *Inorg Chem.* 2004;43:7774–7783.
15. Lipowska M, He H, Xu X, Marzilli LG, Taylor A. First evaluation of a ^{99m}Tc-tricarbonyl complex, ^{99m}Tc(CO)$_3$(LAN), as a new renal radiopharmaceutical in humans. *J Nucl Med.* 2006;47:1032–1040.
16. He H, Lipowska M, Christoforou AM, Marzilli LG, Taylor AT. Initial evaluation of new ^{99m}Tc(CO)$_3$ renal imaging agents having carboxyl-rich thioether ligands and chemical characterization of Re(CO)$_3$ analogues. *Nucl Med Biol.* 2007;34:709–716.
17. Lipowska M, Marzilli LG, Taylor AT. ^{99m}Tc(CO)$_3$-nitrilotriacetic acid: a new renal radiopharmaceutical showing pharmacokinetic properties in rats comparable to those of ^{131}I-OIH. *J Nucl Med.* 2009;50:454–460.
18. Taylor AT, Lipowska M, Marzilli LG. ^{9m}Tc(CO)$_3$-NTA: a ^{99m}Tc renal tracer with pharmacokinetic properties comparable to those of ^{131}I-OIH in healthy volunteers. *J Nucl Med.* 2010;51:391–396.
19. Bhadwal M, Satpati D, Singhal S, et al. Preparation of ^{99m}Tc(CO)$_3$-carboxymethylthioethyl iminodiacetic acid and evaluation as a potential renal imaging agent. *Curr Radiopharm.* 2012;5:65–70.
20. Klingensmith WC III, Fritzberg AR, Spitzer VM, et al. Clinical evaluation of Tc-99m *N, N′*-bis (mercaptoacetyl)-2,3-diaminopropanoate as a replacement for I-131 hippurate: concise communication. *J Nucl Med.* 1984;25:42–48.
21. Taylor A Jr, Eshima D. Effects of altered physiologic states on clearance and biodistribution of technetium-99m MAG3, iodine-131 OIH, and iodine-125 iothalamate. *J Nucl Med.* 1988;29:669–675.
22. Rattat D, Eraets K, Cleynhens B, Knight H, Fonge H, Verbruggen A. Comparison of tridentate ligands in competition experiments for their ability to form a [^{99m}Tc(CO)$_3$] complex. *Tetrahedron Lett.* 2004;45:2531–2534.
23. Anghileri LJ. A simplified method for preparing high specific activity ^{131}I-labeled hippuran. *Int J Appl Radiat Isot.* 1964;15:95.
24. Levey AS, Coresh J, Balk E, et al. National Kidney Foundation practice guideline for chronic kidney disease: evaluation, classification and stratification. *Ann Intern Med.* 2003;139:137–147.

25. Sapirstein LA, Vidt DG, Mandel MJ, Hanusek G. Volumes of distribution and clearance of intravenously injected creatinine in the dog. *Am J Physiol.* 1955;181:330–336.
26. Esteves F, Halkar R, Issa M, et al. Comparison of camera-based Tc-99m MAG3 clearance and the 24 hour creatinine clearance for evaluation of kidney function. *AJR.* 2006;187:W316–319.
27. Chudleigh RA, Dunseath G, Peter R, et al. Influence of body weight on the performance of glomerular filtration rate estimators in subjects with type 2 diabetes. *Diabetes Care.* 2008;31:47–49.
28. Taylor A, Kipper MS. The qualitative I-131 hippuran renogram: a potential problem. *Clin Nucl Med.* 1983;8:149–154.
29. Budny JA, Arnold JD. Nitrilotriacetate (NTA): human metabolism and its importance in the total safety evaluation program. *Toxicol Appl Pharmacol.* 1973;25:48–53.
30. Health Canada. Environmental and Workplace Health. Nitrilotriacetic acid (NTA). 1990. Available at: http://www.hc-sc.gc.ca/ewh-semt/pubs/water-eau/nitrilotriacetic_acid/index-eng.php.
31. World Health Organization. *Nitrilotriacetic Acid in Drinking-Water. Guidelines for Drinking-Water Quality. Health Criteria and Other Supporting Information.* Vol. 2, 2nd ed. Geneva, Switzerland: World Health Organization; 1996.
32. Anderson RL, Bishop WE, Campbell RL. A review of the environmental and mammalian toxicology of nitrilotriacetic acid. *Crit Rev Toxicol.* 1985;15:1–102.
33. Taylor A Jr, Eshima D, Christian PE, Milton W. Evaluation of a new Tc-99m-mercaptoacetyltriglycine in patients with impaired renal function. *Radiology.* 1987;162:365–370.
34. Zuckier LS, Axelrod MS, Wexler JP, Heller SL, Blaufox MD. The implications of decreased performance of new generation gamma-cameras on the interpretation of ^{131}I-Hippuran renal images. *Nucl Med Commun.* 1987;8:49–61.
35. Taylor A, Manatunga A, Morton K, et al. Multicenter trial validation of a camera based Tc-99m MAG3 clearance. *Radiology.* 1997;204:47–54.
36. Esteves FP, Taylor A, Manatunga A, et al. ^{99m}Tc-MAG3 renography: normal values for MAG3 clearance and curve parameters, excretory parameters and residual urine volume. *AJR.* 2006;187:W610–W617.
37. O'Reilly P, Aurell M, Britton K, et al. Consensus on diuresis renography for investigating the dilated upper urinary tract. *J Nucl Med.* 1996;37:1872–1876.
38. Gordon I, Colarinha P, Fettich J, et al. Guidelines for standard and diuretic renogram in children. *Eur J Nucl Med.* 2001;28:BP21–BP30.
39. Shulkin BL, Mandell GA, Cooper JA, et al. Procedure guideline for diuretic renography in children 3.0. *J Nucl Med Technol.* 2008;36:162–168.
40. Taylor AT, Blaufox MD, De Palma D, et al. Guidance document for structured reporting of diuresis renography. *Semin Nucl Med.* 2012;42:41–48.